

Mixed quantum-classical molecular dynamics simulation of vibrational relaxation of ions in an electrostatic field

Andreas D. Koutselos

Physical Chemistry Laboratory, Department of Chemistry, National and Kapodistrian University of Athens, Panepistimiopolis, 15771 Athens, Greece

(Received 30 August 2006; accepted 27 November 2006; published online 29 December 2006)

The vibrational relaxation of ions in low-density gases under the action of an electrostatic field is reproduced through a molecular dynamics simulation method. The vibration is treated through quantum mechanics and the remaining degrees of freedom are considered classical. The procedure is tested through comparison against analytic results for a two-dimensional quantum model and by studying energy exchange during binary ion-atom collisions. Finally, the method has been applied successfully to the calculation of the mobility and the vibrational relaxation rate of O_2^+ in Kr as a function of the mean collision energy using a model interaction potential that reproduces the potential minimum of a previously known *ab initio* potential surface. The calculation of the steady mean vibrational motion of the ions in (flow) drift tubes seems straightforward, though at the expense of large amounts of computer time. © 2006 American Institute of Physics.

[DOI: 10.1063/1.2424457]

I. INTRODUCTION

Combined quantum-classical molecular dynamics (MD) simulation methods have been developed for the study of the vibrational relaxation in gas and condensed phases¹⁻³ among various other applications.^{4,5} They belong to a class of approximation methods in which part of the system is treated through quantum mechanics and the remaining part, often serving as a thermal bath, through classical mechanics. Thus, the quantal excitations appear to be relaxing through the influence exerted by a classical medium, with the latter acquiring the dissipated thermal energy. Among such approaches the mean field (MF) Ehrenfest method has been employed for the study of vibrational relaxation of CN^- in aqueous solution.¹ In addition, this method has been found to outperform the “surface hopping” variant, especially in cases where the probability distribution is not split in contributions that are influenced differently by the environment.⁶ Such conditions are expected to apply to perturbed oscillators, and therefore the approach should be an appropriate candidate for the study of the vibrational motion of ions in the gas phase, within the accuracy of the approximation involved in the (mixing) procedure.

In the following, we present such a mixed quantum-classical MD method for the simulation of the motion of swarms of diatomic ions in gases under the influence of an electrostatic field, with the vibration of the ions treated through quantum mechanics. In addition, since the ions should acquire a drift motion in the gas, an effective mechanism is employed for the extraction of excess thermal energy from the system. This is accomplished through the use of the technique of “images of atoms,”^{7,8} which we have developed in the past and involves the generation of appropriate initial conditions for the gas atoms that interact with the ions. Then, the excess ion energy will be extracted during the simulation

of the ion-neutral collisions uninterruptedly, without the introduction of effective interactions as in the case of other temperature control mechanisms.⁹

The whole procedure should enable the calculation of the dynamics of the vibrational motion and its possible effect on the rotation and translation of the ions. With computer runs of adequate length, the properties of the vibrational degree of freedom and its correlation to the remaining degrees should be probed as a function of the field strength and the gas temperature. Such effects have already been noted in the past as in vibrationally state-selected experiments of CO^+ in He,¹⁰ where the ion seems to be more mobile when it is in the second excited vibration state than in the ground state. An analogous observation has been made for ArH^+ in a He dc glow discharge.¹¹ Furthermore, vibrational relaxation rates of a considerable number of molecular ions have been measured¹²⁻¹⁴ so far and have been analyzed through scattering calculations based on approximate velocity and orientation distributions of the ions. The current procedure, however, is free from such restrictions even at high field strengths, since the ion motion is simulated accurately at nonequilibrium conditions.

Our method is first tested for the Ehrenfest MF evolution of the quantum degree of freedom against a fully quantal model calculation in analogy to the study of Kohen *et al.*⁶ In addition, the energy exchange in binary ion-atom collisions is studied using a model interaction potential. The evolution of the classical degrees of freedom need not be tested since the program has been based on a previously developed computer code which has been developed for the simulation of the motion of rigid molecular ions in electrostatic fields.¹⁵

Finally, the present approach is applied to O_2^+ in Kr, using a site-site model potential that acquires the depth and the geometry of the minimum of an *ab initio* intermolecular potential calculated in the past.¹⁶ Here, we study the reproduc-

tion of the ion mobility experimental data and draw a general conclusion about the accuracy of the interaction potential. In addition, the population relaxation rate of the first excited vibration state of O_2^+ is determined at various field strengths and is compared to results of flow drift tube measurements.

Subsequently, in Sec. II we present the MD method. Then, in Sec. III the quantum-classical mixing procedure is described with modifications pertinent to ion swarm experiments. In Sec. IV, the method is first tested against accurate results for a simple quantum model and subsequently is applied to an actual system (O_2^+ in Kr). Finally, in Sec. V we assess the performance of the method and discuss improvements that can extend its use.

II. NONEQUILIBRIUM MOLECULAR DYNAMICS METHOD

We consider noninteracting homonuclear diatomic ions moving in a low-density gas under the action of an electrostatic field. The gas acts as a thermal bath for the ions extracting their excess energy, which is acquired by the action of the external field, through binary uncorrelated collisions. These considerations are consistent with the usual (flow) drift tube experimental conditions.¹⁷

Under these conditions, the ion-neutral interaction involves an ion and a single neutral atom, and therefore the corresponding Hamiltonian during a collision may be analyzed as follows:

$$H = H_0 + H_C, \quad (1)$$

with

$$H_0 = \frac{p^2}{2\mu} + V_r(r), \quad (2)$$

where r and p are the internuclear separation of the ion and its corresponding momentum, to be treated through quantum mechanics, μ is the reduced mass of the ion, and $V_r(r)$ is the intramolecular potential of the ion. The second term includes gas, ion, and ion-gas contributions,

$$H_C = H_R + H_r, \quad (3)$$

with

$$H_R = \frac{\mathbf{P}_n^2}{2M} + \frac{\mathbf{P}_c^2}{2m} \quad (4)$$

and

$$H_r = \frac{\mathbf{L}^2}{2I(r)} + V(r, \mathbf{R}_n, \mathbf{R}_i), \quad (5)$$

where \mathbf{R}_n and \mathbf{R}_i represent gas and ion coordinates, respectively, to be treated eventually through classical mechanics. The latter consist of the center of mass coordinates \mathbf{R}_c and the two angles $\boldsymbol{\Omega} \equiv (\theta, \phi)$ that orient the ion in space. Also, \mathbf{P}_n and \mathbf{P}_c are the momenta of the gas atom and of the center of mass of the ion, respectively, and M and m are the masses of the corresponding species. The first term on the right hand side of Eq. (5) represents the rotational energy of the ion, with \mathbf{L} and I being the angular momentum and the moment of inertia of the ion. The latter depends on r through $I(r)$

$= \mu(r_m + r)^2$, where r_m is the position of the minimum of V_r . The second term of the above equation involves the ion-atom interactions.

In addition to the sparse ion-neutral interactions, a constant force is applied at the center of mass of the homonuclear ion due to the electric field. Finally, the gas atoms are assumed to interact with one another and to remain always at equilibrium.

To reproduce the ion motion under the above conditions, we extend the use of a nonequilibrium MD method of images of atoms^{7,8,15} that has been developed in the past and has been successfully applied for the study of transport and dynamic properties of the ions in an electrostatic field involving classic degrees of freedom. Since details of the MD method have been presented in the past, it is sufficient here to mention its main features.

Accordingly, the nonequilibrium character of the ion motion is reproduced by simulating ions under the action of an electric field independently of one another (without forces exerted among them), together with their immediate microenvironment consisting of gas atoms that are initially emerging from a parallel running independent equilibrium MD procedure. These images are created as the gas atoms approach an ion at some specific distance and are followed until they move away from the ion. Thus, effectively, the excess energy accumulated to the ion by the external field is continuously dissipated as thermal energy to images of gas atoms without disturbing the equilibrium state of the gas, which anyway is simulated independently of the ions.

In traditional (flow) drift tube experiments the ion transport is characterized mainly by a drift motion and a superposed nonisotropic diffusion with two components, one parallel and one perpendicular to the field. The MD method, likewise, provides the mean velocity of the ions and diffusion coefficients through time integration of relevant velocity autocorrelation functions.¹⁸

To complete the method, one has to employ a procedure that separates and treats the quantum and classical degrees of the system in a consistent way.

III. MIXED QUANTUM-CLASSICAL METHOD

Since the vibration of a diatomic ion in traditional drift tube experiments involves excitation quanta comparable to the mean thermal energy of the ions, eventually energy is stored in the vibrational motion. This may not affect severely the transport of the ions but the ion transport characterizes critically the distribution of the vibrational energy,¹⁹ as well as the vibrational dynamics and the vibrational relaxation rate in quenching experiments.^{13,14}

It thus appears that the vibrational motion should be simulated along with the translational and rotational motions of the ions in a unified treatment. However, the magnitude of the vibrational energy differences requires consideration of the quantum mechanical nature of the motion. To implement this we employ an MF Ehrenfest method²⁰ and treat only the vibration of a diatomic ion through quantum mechanics. The main steps of the method and its variations that have been introduced in our approach are presented below.

In a general formulation, initially all degrees of freedom, r and $\mathbf{R} \equiv \{\mathbf{R}_n, \mathbf{R}_i\}$, are treated as quantum variables and the total wave function $\psi(r, \mathbf{R}, t)$ is analyzed in two factors, each depending explicitly on r and \mathbf{R} variables,

$$\psi(r, \mathbf{R}, t) = \varphi(r, t) \xi(\mathbf{R}, t) e^{i\hbar \int^t E_r(t') dt'}, \quad (6)$$

with the phase defined through

$$E_r(t) = \int \int \varphi^* \xi^* (H_0 + H_r) \varphi \xi d\mathbf{r} d\mathbf{R}. \quad (7)$$

Since the variables r and \mathbf{R} differ, in as much as the first is considered fast and the other slow, the phase is further analyzed asymmetrically through a convenient but arbitrary assumption for the slow variable,²⁰

$$i\hbar \int \xi^* \frac{\partial \xi}{\partial t} d\mathbf{R} = E, \quad (8)$$

with

$$E = \int \int \varphi^* \xi^* H \varphi \xi d\mathbf{r} d\mathbf{R}. \quad (9)$$

This leads then to

$$i\hbar \int \varphi^* \frac{\partial \varphi}{\partial t} d\mathbf{r} = E_r \quad (10)$$

for the fast variable.

The evolution of $\psi(r, \mathbf{R}, t)$ is described by the Schrödinger equation

$$i\hbar \frac{\partial}{\partial t} \psi(r, \mathbf{R}, t) = H \psi(r, \mathbf{R}, t). \quad (11)$$

To obtain the evolution of $\varphi(r, t)$ then, one has to introduce $\xi^*(\mathbf{R}, t)$ in the left hand side of the above equation, integrate over \mathbf{R} , and make use of Eqs. (8) and (10),

$$i\hbar \frac{\partial}{\partial t} \varphi(r, t) = (H_0 + H_r) \varphi(r, t), \quad (12)$$

with H_0 and H_r defined through Eqs. (2) and (5). The first part, H_0 , corresponds to a harmonic oscillator of frequency ω , for convenience. Although more realistic model potentials such as the Morse potential can be used, we prefer at present to employ a potential that can be calculated efficiently and still be accurate when only a few vibrational levels are excited. The term

$$H_r = \frac{\mathbf{L}^2}{2I(r)} + V(r, \mathbf{R}_n, \mathbf{R}_i) \quad (13)$$

is treated as a perturbation to the harmonic oscillator. The first term, introduced before, involves the coupling between the vibration and the rotation of the ion, V-R coupling, and the second is the potential interaction between the ion and the gas atoms.

The solution of the Schrödinger equation can be accomplished through an analysis of the wave function based on harmonic oscillator eigenfunctions $\varphi_n(r)$ of the unperturbed Hamiltonian,

$$H_0 \varphi_n(r) = E_n \varphi_n(r), \quad (14)$$

as follows:

$$\varphi(r, t) = \sum_n c_n(t) e^{-iE_n t/\hbar} \varphi_n(r). \quad (15)$$

In dense media it seems appropriate for the wave function to be analyzed in terms of eigenfunctions of Hamiltonians that depend on the instantaneous position of the classical degrees of freedom (which affect the vibrational motion). As the main features of the vibrational motion are found to be followed well in relaxation studies¹ even when the wave function is analyzed through the use of vacuum eigenfunctions, it seems that this elaborate calculation can also be replaced in less dense environments by the simpler implementation of vacuum reference states. This is so because the ions move most of their time without interacting with the neutrals, and the interactions, whenever they occur, perturb weakly the vibrational motion at least at low and intermediate field strengths in traditional drift tube experiments. This issue is discussed also below. The only additional perturbation to the vibrational motion, coming from the continuous action of the V-R coupling, is expected again to affect the vibration rather weakly.

The introduction of the above expression of $\psi(r, t)$ into Eq. (12) produces a well known equation for the c_n expansion coefficients,

$$i\hbar \frac{d}{dt} c_n(t) = \sum_m H_{nm}^{(1)} e^{-i\omega_{nm} t/\hbar} c_m(t), \quad (16)$$

with

$$H_{nm}^{(1)} = \int \varphi_n^*(r) H_r \varphi_m(r) dr \text{ and } \omega_{nm} = (E_n - E_m)/\hbar. \quad (17)$$

Similarly, in order to obtain the evolution of $\xi(\mathbf{R}, t)$, one has to introduce $\varphi^*(r, t)$ in the left hand side of Eq. (11), integrate over r , and make use of Eqs. (8) and (10),

$$i\hbar \frac{\partial}{\partial t} \xi(\mathbf{R}, t) = \left(H_R + \int \varphi(r, t)^* (H_0 + H_r) \varphi(r, t) dr \right) \xi(\mathbf{R}, t), \quad (18)$$

with the Hamiltonian terms defined through Eqs. (2), (4), and (5).

To proceed further in deriving the classic equations of motion for \mathbf{R} , we define the moment of inertia I_c through the centrifugal term that appears in the above equation by setting

$$\frac{\mathbf{L}^2}{2I_c} = \int \varphi(r, t)^* \frac{\mathbf{L}^2}{2I(r)} \varphi(r, t) dr. \quad (19)$$

Then, through representation of $\xi(\mathbf{R}, t)$ by $A(\mathbf{R}, t) \exp\{iS(\mathbf{R}, t)/\hbar\}$ and taking the limit of \hbar going to zero in Eq. (18), one obtains a Hamilton-Jacobi equation which leads to the usual classic equations of motion,²⁰ expressed in general form,

$$\frac{d\mathbf{P}}{dt} = - \int \varphi(r,t)^* \nabla_{\mathbf{R}} V(r, \mathbf{R}_n, \mathbf{R}_i) \varphi(r,t) d\mathbf{r} = - \langle \nabla_{\mathbf{R}} V \rangle, \quad (20)$$

where \mathbf{R} and \mathbf{P} denote coordinates (collectively, both \mathbf{R}_n and \mathbf{R}_i) and their conjugate momenta. Thus, the translational motion and the ion center of mass coordinates \mathbf{R}_c included in \mathbf{R}_i follows the Newton equation with the forces defined as averages over the quantal vibrational variable. In the case of the angular variables, expressed in body coordinates, \mathbf{P} corresponds to the angular momentum \mathbf{L} and the right hand side to relevant torques. Since, now, the moment of inertia is not constant but varies in time, the time derivative of \mathbf{L} contains two terms,

$$\frac{d\mathbf{L}}{dt} = \dot{I}_c \boldsymbol{\omega} + I_c \dot{\boldsymbol{\omega}}. \quad (21)$$

Here, the rate of change of the moment of inertia \dot{I}_c is calculated from a quantum mechanical average consistent with Eq. (19).

In this treatment the probability of finding the diatomic ion in a vibrational state at certain time is furnished through $P_n = |c_n(t)|^2$, assuming that the expansion in terms of vibrational eigenfunctions of the unperturbed diatom is legitimate at low gas density as explained above. The values of the coefficients, in turn, are obtained as statistical averages in time from an ensemble of ions. Finally, the energy of the vibrational mode, E_V , is given by

$$E_V = \sum_n P_n E_n, \quad (22)$$

and an effective vibrational temperature can be defined from the energy that is stored in this mode above the zero point energy,

$$kT_V = \sum_n P_n (E_n - E_0). \quad (23)$$

Other properties related to the quantal degree of freedom, such as correlations with different molecular modes, can also be determined in principle, though their calculation requires large amounts of computer time.

IV. APPLICATIONS

The procedure involves a quantum-classical mixing procedure for the unified treatment of the vibration and the remaining classic molecular and gas degrees of freedom as well as an effective mechanism for maintaining the ion transport at steady state under the action of an electrostatic field. Since the latter technique has been developed for classical molecular ions and has been tested thoroughly in the past, we proceed to study the simulation of the vibrational motion of the ion.

A. Harmonic oscillator model

The present approach is first tested against results obtained for a simple analytic model to which the present method can be applied directly after the degrees of freedom of the system are reduced to 2. For this purpose, we have modified the program by considering only one homonuclear

diatomic ion to move in one direction, with center of mass coordinate R and (total) mass m , under the action of an external harmonic potential of force constant $K = m\Omega^2$. In addition, the vibration coordinate of the ion, r , represents an oscillator of (reduced) mass μ and force constant $k = \mu\omega^2$ that has to be treated through quantum mechanics in the mixed approach. The overall Hamiltonian then becomes

$$H = \frac{p^2}{2\mu} + \frac{P^2}{2m} + \frac{1}{2}kr^2 + \frac{1}{2}K(r+R)^2, \quad (24)$$

where p and P are momenta of coordinates r and R , respectively. The evolution of this system can be determined easily through a linear transformation to two decoupled harmonic oscillators. The corresponding mixed quantum-classical treatment, however, is tested for two different harmonic oscillator bases, one defined in vacuum and the other as a Born-Oppenheimer (BO) basis defined instantaneously under the external interaction. The first set of eigenfunctions corresponds to force constant $k+K$, when the potential energy of the Hamiltonian is rewritten in the form

$$V = \frac{1}{2}(k+K)r^2 + KrR + \frac{1}{2}KR^2. \quad (25)$$

The second and third terms on the right hand side of this equation are treated as perturbations to the harmonic oscillator which is represented by the first term. The BO basis, on the other hand, is based on another analysis of the potential energy,

$$V = \frac{1}{2}(k+K) \left(r + \frac{k}{k+K} R \right)^2 + \frac{1}{2} \frac{kK}{k+K} R^2, \quad (26)$$

and requires consistent treatment of the evolution of $\psi(r, R, t)$ [Eq. (6)]. In this case, R is treated as a slow-varying coordinate that modifies continuously the oscillator eigenstates. Although the second set is more appropriate for strongly interacting systems, the first one is more convenient and equally accurate in weakly interacting systems.

Detailed testing has shown that the present program reproduces the analytic results for both bases with the accuracy expected from the study of the mixing method by Kohen *et al.*⁶ The most interesting calculated quantity is the probability of finding the internal harmonic oscillator at an (here vacuum) eigenstate. This probability for the ground state is plotted with respect to time in Fig. 1, for an internal oscillator starting from the ground state. In the mixed approach the slow oscillator has been displaced at the turning point of the ground state energy, R_0 , and in the quantum mechanical treatment it has been represented initially through a Gaussian wave packet centered at R_0 , with width $\sigma = R_0$. We find that despite the difference between the mean field and the fully quantum results, which is exemplified here due to the unfavorable conditions for the separation of the coordinates, since the masses of the oscillators are not very different in magnitude, $\mu/m = 0.25$, the former follow closely the main variations of the latter in time.

The two simulation results, one obtained by employing a vacuum basis and the other by using interaction (BO) states, appear in Fig. 1 to be almost identical even with the use of coupling constants of high magnitude. In the following we

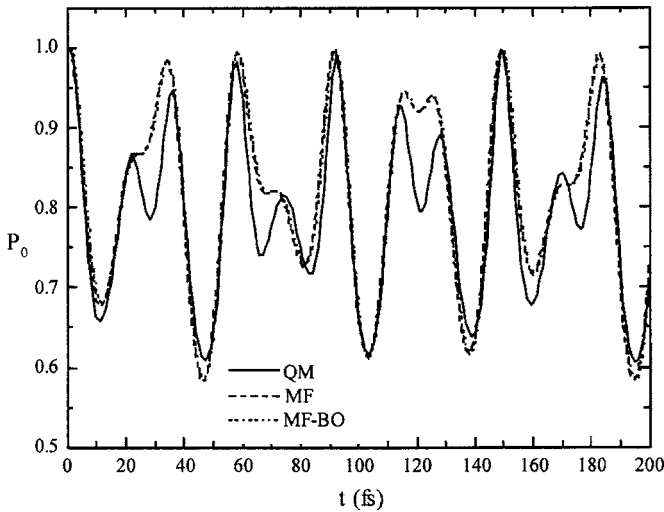


FIG. 1. Population of the ground oscillator state in time with $\omega=2\Omega=1000\text{ cm}^{-1}$. The solid line is the result of the analytic calculation. The dashed line is the mean field result with vacuum basis. The dotted line is also a mean field result but with a BO basis.

employ the former basis as it is most convenient and expect the approach to be adequate for interactions in the gas state at least up to intermediate field strengths.

B. Energy exchange under the action of an electric field

Before applying the current method to an actual system we have studied the energy variation during binary O_2^+-Kr encounters under the action of an electrostatic field. Although there are a few model ion-atom potentials^{21–23} and an *ab initio* potential surface presented in the literature,¹⁶ we prefer to employ here a site-site 12-6-4 model potential to describe the ion-atom interaction because it is more efficient for the calculations and is accurate at large separations. The minimum of the model potential, however, is forced to appear at the minimum of the *ab initio* potential, which has been located at distance $R_m=3.10\text{ \AA}$ of Kr from the center of mass of O_2^+ , at depth $E=0.173\text{ eV}$ and at O–O–Kr angle $\delta=139^\circ$.

The total interaction potential acquires the form

$$V = V_1(R_1) + V_2(R_2), \quad (27)$$

with the site-site (O–Kr) contributions given by

$$V_i(R_i) = \frac{E_i}{2} [(1 + \gamma_i)(R_{m,i}/R_i)^{12} - 4\gamma_i(R_{m,i}/R_i)^6 - 3(1 - \gamma_i) \times (R_{m,i}/R_i)^4],$$

where R_i are the distances of Kr from the i th O site. The two sets of $(E_i, R_{m,i})$ parameters, representing the depths and the positions of the minima of V_i , should differ from one another in order for the global minimum of V to be located at the asymmetrical position of the *ab initio* result. The R_m 's are found to be $R_{m,1}=2.784\text{ \AA}$ and $R_{m,2}=3.480\text{ \AA}$, when $R_1 \leq R_2$. For the remaining region the values of the parameters have to be interchanged. The depths are constrained through $E_1 + E_2 = E$, and are assumed to be related through the polarization form of the potential, $E_i \propto R_i^{-4}$, around the minimum.

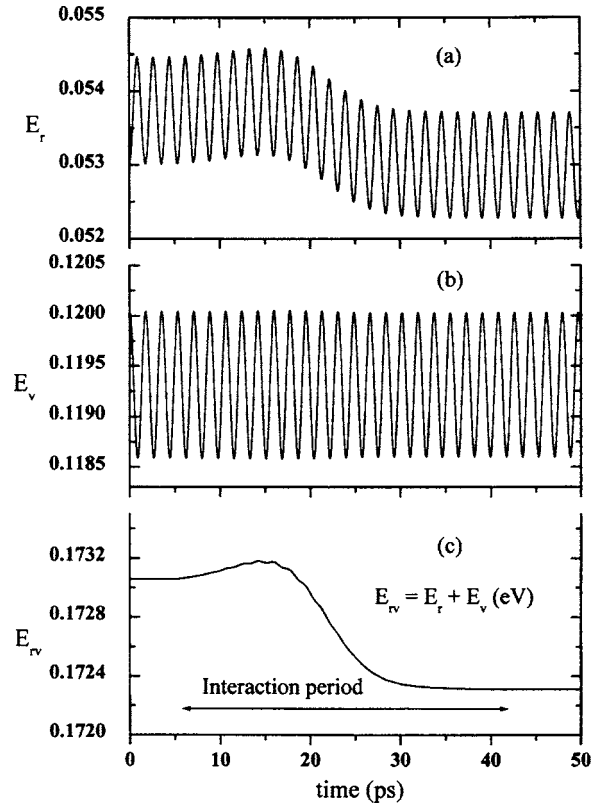


FIG. 2. Ion energy contributions during an ion-atom collision as presented in the text. (a) Rotational energy. (b) Vibrational energy. (c) Summed rotational and vibrational energies.

That is, $E_1 R_{m,1}^4 = E_2 R_{m,2}^4$. The obtained depths are $E_1 = 0.1227\text{ eV}$ and $E_2 = 0.0503\text{ eV}$. Finally, the gamma parameters are calculated by requiring the long-range part of the potential to match the polarization limit, that is, assuming $V_1 \approx V_2$ at large R ,

$$3E_i(1 - \gamma_i)(R_{m,i}/R_i)^4 = e^2 a_d / 2R_i^4, \quad (28)$$

where a_d is the dipole polarizability of Kr. The resulting values are $\gamma_1 = \gamma_2 = 0.1921$. Finally, for Kr we employ an accurate Lennard-Jones potential with $E=171\text{ K}$ (or 0.01474 eV) and $\sigma=3.60\text{ \AA}$.²⁴ The value of the internuclear separation and vibrational frequency of O_2^+ have been set equal to the experimental values of 1.117 \AA and 1876.4 cm^{-1} ,^{25,26} respectively.

Using the above interaction potentials we can simulate an ion-atom encounter and monitor the energy transfer among various degrees of freedom. Most of the time the motion of the center of mass of an ion is purely accelerating, and from time to time the motion is disturbed for a short period by the approach of a gas atom. In Figs. 2 and 3 we present various energy contributions for an ion-atom encounter at 3 eV collision energy, with 6 \AA impact parameter and the ion initially set in the ground oscillator state. The electric field strength over the gas number density, E/N , is 600 Td , ($1\text{ Td}=10^{-21}\text{ V m}^2$). It is seen that during the free flight of the ion, before and after the interaction period, both rotation and vibration energies oscillate vividly [Figs. 2(a) and 2(b)], while their sum remains constant in time [Fig. 2(c)]. Numerically, this energy conservation holds within seven significant

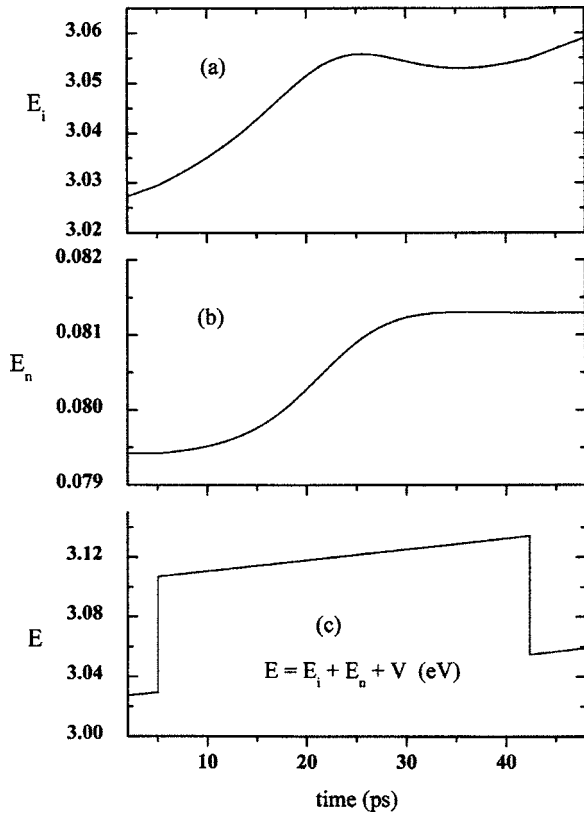


FIG. 3. Ion and atom energy contributions during a collision, as in Fig. 2. (a) Total ion kinetic energy. (b) Translational energy of the atom. (c) Summed ion and atom energy including the potential energy during the interaction period denoted in Fig. 2(c).

figures. In this stage, the relevant total ion energy, which includes translation, vibration, and rotation contributions ($T + V + R$), increases in time due to the action of the electric field [Fig. 3(c)].

When the ion-atom interaction starts, a redistribution of the energies of the particles takes place. We observe in Figs. 2(a) and 2(b) a change of V and R energies of the ion and a variation with a final decrease of their sum, ($V + R$), in Fig. 2(c). Furthermore, in Fig. 3(a) a decrease of the total ion energy is noticed due to the interaction of the ion with the gas atom. This change becomes vivid if one extrapolates the initial part of the graph and compares it to its final part. The gas atom, in turn, acquires the energy from the ion as seen in Fig. 3(b). However, during the interaction the sum of the ion and atom energies increases due to the action of the field [Fig. 3(c)]. The abrupt change in the total energy in this figure is due to the temporary addition of the translation energy of the atom to the energy of the ion during the interaction period.

By comparing the initial part of the total ion energy to the final one in Fig. 3(c), we see that in this collision, despite the transfer of the energy from the ion to the neutral, the total energy of the ion has been increased due to the action of the electric field. In general, however, the ions are slowed down during collisions by transferring continually part of their energy to the neutral atoms.

It is pleasing to see that all parts of the energy vary consistently under the action of an electric field though only

one degree of freedom is treated through quantum mechanics. We can now proceed to the study of the transport and vibrational relaxation of a swarm of ions.

C. Kinetic properties of O_2^+ in Kr

The simulation proceeds in four stages. In the first stage, the simulation of the motion of 108 Kr atoms is initiated and followed in an independent MD procedure. When the state of the gas relaxes to equilibrium at 300 K, the simulation of 500 ions is initiated and followed in a second parallel MD procedure, as described in Sec. II. In this (second) stage the ions are forced to acquire certain mean kinetic energies parallel and perpendicular to the field through the use of an effective temperature control scheme. In a third stage the ion transport relaxes unconstrained to its nonequilibrium drift state, and in a final stage, which lasts for about 80% of the whole procedure, statistical averages are calculated by collecting values in time from all ions. At the beginning of the last stage the initial vibration state of the ions is reinstated, though it is only slightly modified during the preceding stages of the simulation. In total, the motion of the ions are followed for about 5×10^7 time steps of 5×10^{-17} s.

Here, we have calculated the mobility, the mean kinetic energies and the population of the ground vibration state of the ion at various electric field strengths. Specifically, the first two moments of the velocity distribution produce the drift velocity v_d and the effective temperatures parallel, T_{\parallel} , and perpendicular, T_{\perp} , to the field (assumed in the Z direction), while the second moments of the angular velocity distribution produce an effective temperature T_r for the rotation through

$$v_d = \langle v_z \rangle,$$

$$\frac{1}{2}kT_{\parallel} = \frac{m}{2}(\langle v_z^2 \rangle - \langle v_z \rangle^2),$$

$$(29)$$

$$\frac{1}{2}kT_{\perp} = \frac{m}{4}(\langle v_x^2 \rangle - \langle v_x \rangle^2 + \langle v_y^2 \rangle - \langle v_y \rangle^2),$$

$$\frac{1}{2}kT_r = \frac{1}{4}(I_{XX}(\langle w_x^2 \rangle - \langle w_x \rangle^2) + I_{YY}(\langle w_y^2 \rangle - \langle w_y \rangle^2)),$$

where the brackets indicate statistical averages, v_i and w_i are ion velocity and angular velocity components, the latter referring to rotations perpendicular to the molecular axis, and I_{ii} are the moments of inertia of the ion.

The mobility is obtained from $K = v_d/E$ and is presented reduced to the standard gas density through $K_O = KN/N_O$, where $N_O = 2.686763 \times 10^{25} \text{ m}^{-3}$ is Loschmidt's constant and N is the gas number density. The rather steady behavior of K_O in time has shown that the vibrational relaxation has little effect on the kinetic properties of the ions. Although a time correlation between the vibration and the rest of the degrees of freedom may exist, the transport properties appear insensitive to the vibrational excitation at low-density drift tube experimental conditions.

The mobility has been calculated with 2% uncertainty and is presented in Fig. 4 together with measured mobilities at various field strengths.^{27,28} It seems that the interaction

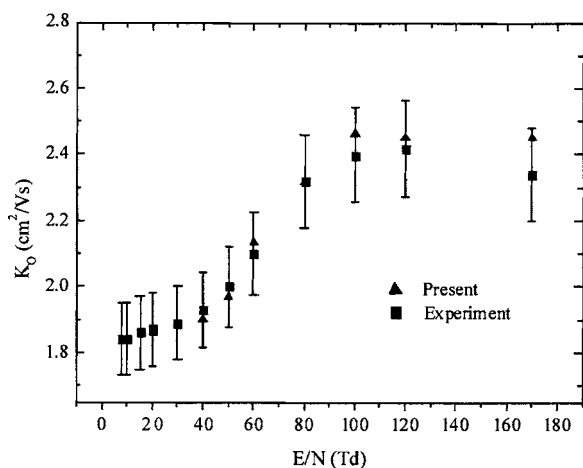


FIG. 4. Normalized mobility at various field strengths. Triangles are present simulation results. Boxes represent experimental data with 6% error bars.

potential reproduces quite accurately the experimental data, since the observed differences are below the experimental error of 6%. However, since the model potential depends on a few empirical parameters, which were evaluated effectively and affect the calculations variably, the observed conformity may be fortuitous. There are actually indications that the *ab initio* potential may be too shallow. Experimental fluorescence dissociation studies²⁹ have produced a depth of 0.33 ± 0.1 eV, which is quite deeper than the *ab initio* result. In addition, plots of VR^4 ought to approach $-e^2 a_d/2$ at large R from below. However, VR^4 remains larger than the limiting value in most geometric arrangements, with bigger discrepancies observed as Kr approaches the center of mass of O_2^+ perpendicularly to its axis. These considerations indicate that the interaction potential may be deeper than the *ab initio* one. Such a change in the potential depth would modify the reproduction of the experimental mobility data through our simulation method. Then, compensation to any such modification has to come from changes of the remaining potential parameters which determine the location of the minimum of the potential. In general, such assertions depend on the ability of the inversion of the mobility to produce a unique interaction potential between a diatomic ion and an atom.

The obtained effective temperatures calculated within 5% are presented in Fig. 5 as a function of E/N . We observe that the rotation temperature lies close to the mean translational temperature $T_{tr} = (T_{\parallel} + 2T_{\perp})/3$, at least up to intermediate field strengths of about 120 Td, as expected on the basis of a kinetic theory analysis.³⁰ At the highest tested field value the coincidence is at the edge of the combined uncertainty of both quantities.

The approach of the two temperatures has also a physical interpretation. Since both the translation and the rotation of the ion exchange energy efficiently only with the translational motion of a structureless gas atom during collisions, the two degrees of freedom should reach an equilibrium with one another, and therefore $T_r \approx T_{tr}$. This should hold at least up to intermediate field strengths.

D. Vibrational relaxation of O_2^+ in Kr

Although the ion transport appears rather insensitive to the vibrational relaxation, the latter depends drastically on

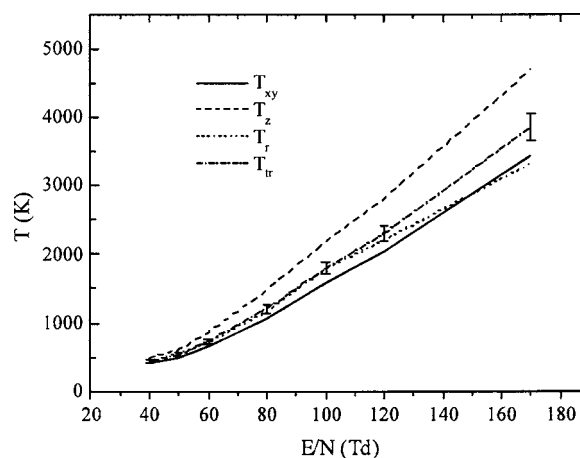


FIG. 5. Effective temperatures for the ions at various field strengths. The solid line is the translational temperature perpendicular to the field, $T_{xy} \equiv T_{\perp}$. The dashed line is a similar temperature along the direction of the field, $T_z \equiv T_{\parallel}$. The dotted line is the rotational temperature T_r . The dash-dot line is the mean translational temperature, $T_{tr} = (T_{\parallel} + 2T_{\perp})/3$, with 5% error bars.

the nonequilibrium motion of the ion. This is seen in Fig. 6, where calculated and experimental vibration relaxation rates^{12,31} are plotted with respect to the mean collision energy, $\frac{3}{2}kT_{\text{eff}} = \frac{3}{2}kT + \frac{1}{2}Mv_d^2$, where M is the mass of Kr. The present results are found to lie constantly above the experimental data, as in the case of previous classical and semi-classical approaches.^{21,22} However, the method reproduces the main qualitative feature of the minimum of the rate coefficient. This nonmonotonic behavior has been interpreted in the past through phenomenological considerations^{13,14} and analyzed semiquantitatively through classical and quantum mechanical treatments.^{21,22,32-34} It has been suggested that at low T_{eff} the vibration relaxation is assisted by the formation of a weak transient complex. At high T_{eff} the direct ion-atom collision process seems to dominate the relaxation process.

The statistical averages of such results depend on pre-assumed velocity and orientation distributions which in general

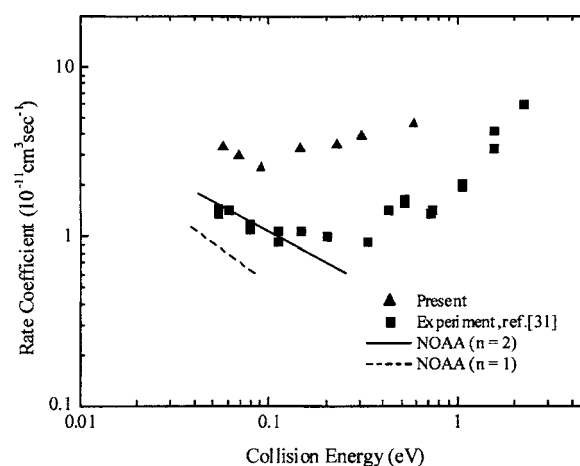


FIG. 6. Vibrational relaxation rate coefficient at various mean collision energies. Triangles are present mixed quantum-classical results. The squares are experimental data with relative initial population $P_2/P_1 \approx 3$ (Ref. 31). The solid line represents NOAA experimental results for initial ion population at $n=2$. The dotted line are also NOAA results with ions at $n=1$ (Ref. 12).

can be approximated well only close to equilibrium. The present method is free from such approximations since it produces the mean translational and rotational motions and the associated dynamics of the ions accurately even at high electric field strengths. The vibrational motion, however, is treated through a mean field quantum approach which should be most accurate at low vibrational excitation. Even so, a detailed analysis of the relaxation mechanism through our method requires long computer runs, especially due to the fact that at small T_{eff} (or field strength), the ion-atom collision rates decrease. Results along this line are deferred to future studies.

V. CONCLUSIONS

A mixed quantum-classical MD method is presented for the simulation of the vibrational motion of swarms of ions moving in gases under the action of an electrostatic field. The method has been constructed through the introduction of a quantum vibrational degree of freedom in a previously designed MD method for rigid rotors. Comparisons against analytic model results show conformity to the results of Kohen *et al.*⁶ from tests of a similar mean field approach.

The application of our method for O_2^+ in Kr, using a 12-6-4 site-site model potential that has been forced to fit an *ab initio* interaction potential around the minimum and acquires the right polarization long-range limit, is found to reproduce quite well the experimental mobility data available in the literature. In addition, the relaxation rate of the first vibration state is calculated for various field strengths and is found to lie close to measured relaxation rates at the edge of the combined experimental and calculation uncertainty.

Improvements for accommodation of higher vibration excitation energy can be implemented easily by employing a Morse O_2^+ intramolecular potential and time evolving (BO) vibration states. The method can furnish additionally the mean vibration energy as well as the correlations between the vibration and the other molecular degrees of freedom.

ACKNOWLEDGMENTS

The author would like to thank the Computer Center of the National and Kapodistrian University of Athens. This work was supported by grants from the Research Fund of the National and Kapodistrian University of Athens (No. 70/4/6482).

- ¹T. Terashima, M. Shiga, and S. Okazaki, *J. Chem. Phys.* **114**, 5663 (2001).
- ²M. F. Herman and J. C. Arce, *Chem. Phys.* **183**, 335 (1994).
- ³M. Head-Gordon and J. C. Tully, *J. Chem. Phys.* **103**, 10137 (1995).
- ⁴J. C. Tully, in *Modern Methods for Multidimensional Dynamics Computation in Chemistry*, edited by D. L. Thompson (World Scientific, Singapore, 1998), Chap. 2.
- ⁵M. F. Herman, *Annu. Rev. Phys. Chem.* **45**, 83 (1994).
- ⁶D. Kohen, F. H. Stillinger, and J. C. Tully, *J. Chem. Phys.* **109**, 4713 (1988).
- ⁷A. D. Koutselos, *J. Chem. Phys.* **102**, 7216 (1995).
- ⁸G. Balla and A. D. Koutselos, *J. Chem. Phys.* **119**, 11374 (2003).
- ⁹D. J. Evans and G. P. Morriss, *Statistical Mechanics of Nonequilibrium Liquids* (Academic, London, 1990).
- ¹⁰E. B. Anthony, M. J. Bastian, V. M. Bierbaum, and S. R. Leone, *J. Chem. Phys.* **112**, 10269 (2000).
- ¹¹N. N. Haese, F.-S. Pan, and T. Oka, *Phys. Rev. Lett.* **50**, 1575 (1983).
- ¹²H. Bohringer, M. Durup-Ferguson, D. W. Fahey, F. C. Fehsenfeld, and E. E. Ferguson, *J. Chem. Phys.* **79**, 4201 (1983).
- ¹³E. E. Ferguson, *J. Phys. Chem.* **90**, 731 (1986).
- ¹⁴W. Lindinger, *Int. J. Mass Spectrom. Ion Process.* **80**, 115 (1987).
- ¹⁵A. D. Koutselos and J. Samios, *Pure Appl. Chem.* **76**, 223 (2004).
- ¹⁶B. Ramiro-Diaz, P. Wahnon, and V. Sidis, *J. Chem. Phys.* **104**, 191 (1996).
- ¹⁷E. A. Mason and E. W. McDaniel, *Transport Properties of Ions in Gases* (Wiley, New York, 1988).
- ¹⁸A. D. Koutselos, *J. Chem. Phys.* **104**, 8442 (1996).
- ¹⁹W. Federer, H. Ramlar, H. Villinger, and W. Lindinger, *Phys. Rev. Lett.* **54**, 540 (1985).
- ²⁰J. C. Tully, in *Classical and Quantum Dynamics in Condensed Phase Simulations*, edited by B. J. Berne, G. Cicciotti, and D. F. Coker (World Scientific, Singapore, 1998), p. 489.
- ²¹P. Tosi and M. Ronchetti, *Chem. Phys. Lett.* **136**, 398 (1987).
- ²²G. Ramachandran and G. S. Ezra, *J. Chem. Phys.* **97**, 6322 (1992).
- ²³E. A. Gislason and E. E. Ferduson, *J. Chem. Phys.* **87**, 6474 (1987).
- ²⁴J. A. Beattie, R. J. Barriault, and J. S. Brieley, *J. Chem. Phys.* **20**, 1613 (1952).
- ²⁵P. H. Krupenie, *J. Phys. Chem. Ref. Data* **1**, 423 (1972).
- ²⁶G. Herzberg, in *Molecular Spectra and Molecular Structure* (Krieger, Malabar, FL, 1989), Vol. 1.
- ²⁷D. R. Lamm, R. D. Chelf, J. R. Twist, F. B. Holleman, M. G. Thackston, F. L. Eisele, W. M. Pope, I. R. Gatland, and E. W. McDaniel, *J. Chem. Phys.* **79**, 1965 (1983).
- ²⁸H. W. Ellis, M. G. Thackston, E. W. McDaniel, and E. A. Mason, *At. Data Nucl. Data Tables* **31**, 113 (1984).
- ²⁹M. F. Jarrold, L. Misy, and M. T. Bowers, *J. Chem. Phys.* **81**, 4369 (1984).
- ³⁰L. A. Viehland, S. L. Lin, and E. A. Mason, *Chem. Phys.* **54**, 341 (1981).
- ³¹M. Kriegl, R. Richter, P. Tosi, W. Federer, W. Lindinger, and E. E. Ferguson, *Chem. Phys. Lett.* **124**, 583 (1987).
- ³²P. Tosi, M. Ronchetti, and A. Lagana, *J. Chem. Phys.* **88**, 4814 (1988).
- ³³E. M. Goldfield, *J. Chem. Phys.* **97**, 1773 (1992).
- ³⁴M. Cramer, S. K. Pogrebnya, and D. C. Clary, *J. Chem. Phys.* **111**, 1972 (1999).